Available online at www.sciencedirect.com
SCIENCE DIRECT
Journal of the European Ceramic Society 26 (2006) 2777–2783
www.elsevier.com/locate/jeurceramsoc

A mechanism for low-temperature sintering

Matjaz Valant [a,*], Danilo Suvorov [a], Robert C. Pullar [b], Kumaravinothan Sarma [b], Neil McN. Alford [b]

[a] *Advanced Materials Department, Jozef Stefan Institute, Jamova 39, 1000 Ljubljana, Slovenia*
[b] *Centre for Physical Electronics and Materials, Faculty of Engineering, Science and the Built Environment (FESBE), London South Bank University, 103 Borough Road, London SE1 0AA, UK*

Received 20 April 2005; received in revised form 30 May 2005; accepted 4 June 2005
Available online 22 August 2005

Abstract

We explain the basic mechanism of the low-temperature sintering called reactive liquid-phase sintering. The mechanism involves the presence of a low-temperature liquid phase that must be able to directly or indirectly accelerate a reaction with the matrix phase. The mechanism is explained in details for the case of the low-temperature sintering of $BaTiO_3$, which was sintered to more than 95% of relative density in 15 min at 820 °C. We have applied reactive liquid-phase sintering to a number of different compounds with very different crystal-chemistry characteristics, and managed to sinter them as much as 400 °C below their original sintering temperatures. A thorough understanding of this sintering mechanism makes it possible to closely control the sintering behavior.

Keywords: Sintering; Perovskites; $BaTiO_3$ and titanates; Capacitors; LTCC

1. Introduction

Until recently, the rapid developments in semiconductor technology have not been matched by the progress in passive components. This situation was especially critical for the telecommunications industry, where the miniaturization of handset devices plays a key role. An important breakthrough came with the introduction of low-temperature cofired ceramic (LTCC) technology, which has enabled miniaturization, the integration of passive functions and a reduction in costs, and has led to the production, for example, of the well-known Bluetooth module. LTCC modules are produced by co-firing ceramic layers with a three-dimensional Ag-microstrip circuitry. To avoid melting of the Ag-microstrips the firing temperature must be around 900 °C, which is extremely low for a ceramic material and represents the major problem with this technology. For a variety of different reasons lowering the sintering temperature is also important for many other technologies, which means it represents the same challenge for other functional materials, e.g. capacitor materials (the production of a base-metal electrode capacitor), piezo-materials (the reduction of Pb losses), etc.

A number of material-research laboratories have focused their research on reducing the sintering temperatures of functional materials. However, because of the lack of fundamental knowledge about low-temperature sintering mechanisms researchers are forced to apply specific empirical principles for each particular material. Only a few attempts to explain the basic mechanisms of low-temperature sintering have been published so far,[1–4] and no general principles have been described.

Many researchers have already investigated the low-temperature sintering of $BaTiO_3$-based ceramics, however, they did not so far clearly explain all the reaction and sintering mechanisms involved in the process.[1,2,5–7] As a rule, the investigators used lithium-fluorite salts as a sintering aid and agreed about the mechanism of incorporating the lithium into the titanium sites of $BaTiO_3$. They assigned an important role in the reduction of the sintering temperature to fluorine ions,

* Corresponding author. Tel.: +386 1 477 3547; fax: +386 1 477 3875.
E-mail address: matjaz.valant@ijs.si (M. Valant).

0955-2219/$ – see front matter © 2005 Elsevier Ltd. All rights reserved.
doi:10.1016/j.jeurceramsoc.2005.06.026

either through the incorporation into the oxygen sublattice or the formation of the low-temperature flux. The composition of the flux has not been determined yet, and the investigators have not explained a peculiar correlation between the stoichiometry of the $BaTiO_3$ and the low-temperature sintering behavior, which was observed during these studies.

Here we explain the fundamental low-temperature sintering mechanism and show that if a few general conditions are ensured then almost any powder can be sintered at temperatures as much as 400 °C lower than its initial sintering temperature. We first determined these conditions for the case of $BaTiO_3$, explained the low-temperature sintering mechanism and showed that no fluorine ions are needed for successful low-temperature sintering. The generalization of the mechanism to other systems with significantly different crystal-chemistry characteristics involved a second research phase.

2. Experimental procedure

Our experiments were carried out using commercial and in-house synthesized powders with a variety of particle sizes: from hydrothermally prepared nano-size particles to micrometer-size particles. The commercial powders were $BaTiO_3$ (Cabot and Alfa Aesar), $(Ba_{0.6}Sr_{0.4})TiO_3$ (PI-KEM LTD, HSB 3000), $SrTiO_3$ (Alfa Aesar), TiO_2 (Alfa Aesar) and X7R (Epcos). The in-house synthesized powders (Zn_2SiO_4 and $AgNbO_3$) were prepared from stoichiometric amounts of corresponding reagent-grade oxides or carbonates. The synthesis was finished when X-ray diffraction analysis showed no secondary phases and the SEM analysis on a sintered sample showed a single-phase composition. The calcined powders were milled for 0.5 h at 200 rpm in a planetary mill using YSZ milling media. The particle size distribution after milling was determined to be mono-modal with an average particle size of 0.7 μm.

The sintering aids were added in the form of water or acetic solutions, thoroughly homogenized and pre-reacted at 600 °C. After a pre-reaction the powders were milled to obtain the mono-modal particle size distribution with an average particle size of 0.7 μm. Such powders were compacted and sintered. The sintering behavior and the activation energy were monitored with a dilatometers (Netzsch 402 C and STA 409) and the reaction mechanisms were followed using powder X-ray diffraction (XRD–Bruker AXS D4 Endeavor) and a thermal analysis system coupled with a quadropole mass spectrometer (Thermostar GSD 300T Baltzers). Evolved-gas analyses (EGA) were performed on CO_2^+, H_2O^+ and Li^+ fragments. The final microstructural characteristics were investigated on the sintered samples using the scanning electron microscope (SEM–Jeol, JXA 840) equipped with TRACOR software (Model TRACOR, Series II X-ray Microanalyzer, Tracor) and transmission electron microscope (TEM–Jeol 2010).

3. Results and discussion

3.1. Low-temperature sintering of $BaTiO_3$

We performed the sintering experiments involving $BaTiO_3$ on a variety of different $BaTiO_3$ powders, whose original sintering temperature is from 1250 to 1300 °C. A small addition of 0.3 wt.% Li_2O was used as a sintering aid in the form of either polycrystalline Li_2O, Li_2CO_3 or an acetic solution of Li^+ ions. The reaction between the dopant and the matrix phase was studied and results showed that the mechanism was exactly the same in all cases. The first reaction between Li_2O and $BaTiO_3$ occurred during the pre-reaction at 600 °C:

$$BaTiO_3 + Li_2O + CO_2 \rightarrow BaCO_3 + Li_2TiO_3$$

When such a pre-reacted powder is milled, compacted and sintered a low-temperature sintering with very high kinetics is experienced. The powder sinters to more than 95% of theoretical density after 15 min at 820 °C (Fig. 1A). Microstructural investigations of the sintered bodies showed the presence of a small concentration of two secondary phases: Li_2TiO_3 and Ba_2TiO_4.

As the melting points of the compounds and the possible eutectics in this system are much higher than the sintering temperature and no significant grain growth was observed, it is not immediately apparent that the sintering is promoted by the presence of a liquid phase. However, the steepness of the sintering curves suggests on some degree of liquid phase sintering. We have used the conventional and high-resolution TEM to investigate a number of the grain boundaries for a presence of the grain-boundary phase that can cause the liquid-phase sintering. All the grain boundaries and triple points were found to be perfectly clear, which can be seen in Fig. 1B and C. To understand this unusual sintering behavior a detailed investigation of the reaction mechanism of the sintering was performed. The sintering process was kinetically frozen at different stages to perform a phase analysis using X-ray powder diffraction (Fig. 2) and differential thermal analyses coupled with evolved-gas analysis (Fig. 3). The analysis showed that the following processes occur during the sintering:

(i) $BaCO_3$ that formed during the pre-reaction melts (melting point of $BaCO_3$ is 811 °C),
(ii) $BaCO_{3(liq)}$ reacts with Li_2TiO_3 to form Ba_2TiO_4 and release Li_2O and CO_2
(iii) LiO_2 incorporates in $BaTiO_3$, according to refs.[1,2,7–9]:

$$2Ti_{Ti}^{x} + 4O_O^{x} + Li_2O \rightarrow 2Li_{Ti}^{'''} + 3V_O^{\bullet\bullet} + O_O + TiO_2$$

(iv) $2BaCO_{3(liq)} + TiO_2 \rightarrow Ba_2TiO_4 + CO_2$
(v) The compact sinters with very fast kinetics. During the reaction the transient liquid phase is consumed and, therefore, no grain-boundary phase can be found.

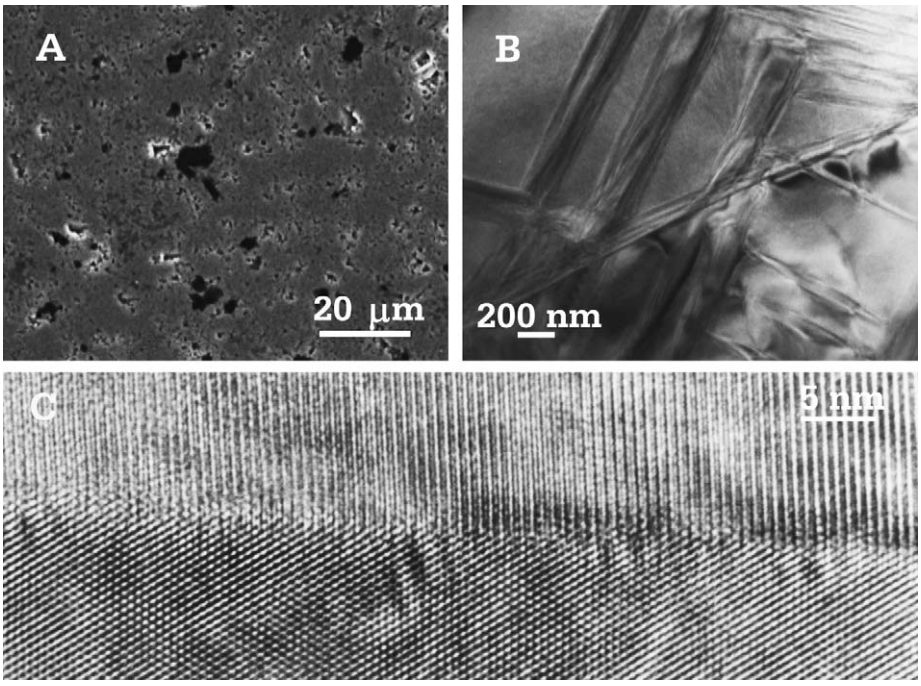

Fig. 1. Electron-microscopy images of $BaTiO_3$ ceramics sintered with the addition of 0.3 wt.% of Li_2O at 820 °C for 15 min. (A) Back-scattered electron image showing the presence of two secondary phases (black phase = Li_2TiO_3, dark gray phase = Ba_2TiO_4) and low residual porosity; (B) scanning TEM image of typical grain boundaries and triple points—no residuals of the liquid phase during the sintering can be seen; (C) high-resolution TEM image of the typical grain boundary, again clean of the residuals of the liquid phase.

To calculate the activation energy (E_a) for the sintering of $BaTiO_3$ powder doped with 0.3 wt.% Li_2O, it was uniaxially pressed (50 Mpa) in an 8 mm die to form pellets with a height of 4 mm. The pellets were then placed in a dilatometer and sintered to a temperature of 1100 °C using varying sintering rates, $k = 5,10,15$ and 20 K min^{-1}. The shrinkage (dL/L_0) of the pellets was measured against temperature (Fig. 4), and the values of dL/L_0 and temperature taken at 3, 6, 9, 12, and 15% shrinkage for each run at heating rate k. Then, for each specific value of shrinkage, ln k was plotted against the inverse of temperature in Kelvin, $1/T$.[10] The experimental determination of E_a was calculated using the Arrhenius expression given below[11]:

$$\ln k = \frac{-E_a}{R}\left[\frac{1}{T}\right] + \ln Z$$

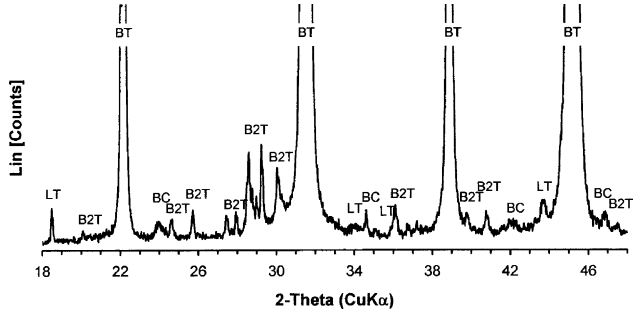

Fig. 2. The X-ray powder diffraction pattern of the of $BaTiO_3$ with the addition of 0.3 wt.% of Li_2O fired at 750 °C for 5 h (BT = $BaTiO_3$, LT = Li_2TiO_3, B2T = Ba_2TiO_4, BC = $BaCO_3$).

where the activation energy (E_a) will be the slope of the graph of ln k against $1/T$ multiplied by the gas constant, R (= 8.3145 J K^{-1} mol^{-1}) (Fig. 5).

The results, calculated from the dilatometric curves, give an average E_a of 586.4 and ±175.8 kJ mol^{-1} for undoped $BaTiO_3$ and an average E_a of 373.8 and ±89.0 kJ mol^{-1} for doped $BaTiO_3$ and again demonstrate the significantly higher sintering kinetics obtained by the doping with Li_2O.

Two further experiments were conducted to reveal the key elements of the fast sintering kinetics. The intention of the experiments was to separately exclude two important substances, which are involved in the proposed reactive

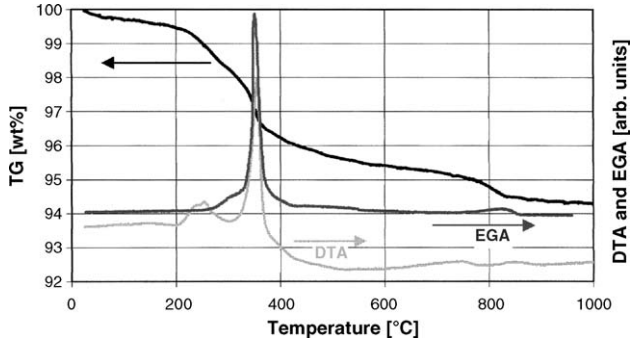

Fig. 3. DTA, TG and EGA of the $BaTiO_3$ with the addition of 0.3 wt.% of Li_2O and a heating rate of 5 K/min. In the temperature range from 200 °C to 400 °C the Li-acetate decomposes with a release of CO_2. CO_2 again evolves at around 800 °C where the reactions of $BaCO_3$ with Li_2TiO_3 and TiO_2 take place.

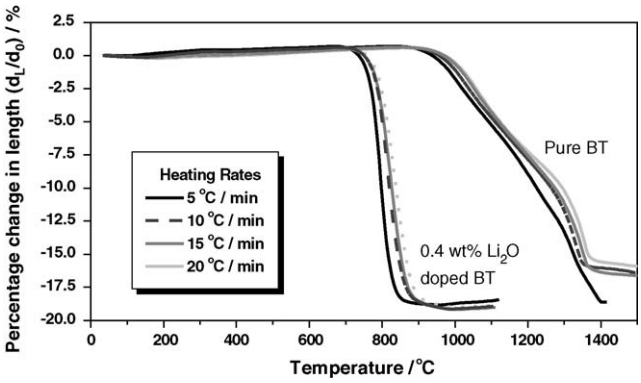

Fig. 4. The shrinkage plots of the pure and Li-doped BT powders, measured at heating rate of 5, 10, 15 and 20 °C min^{-1}.

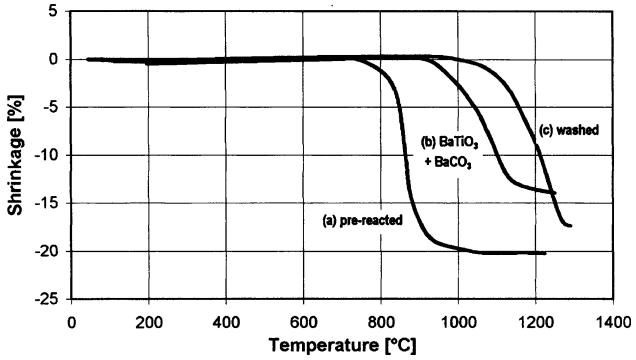

Fig. 6. Dynamic sintering curves (heating rate of 10 K/min) of the $BaTiO_3$ powder with addition of 0.3 wt.% Li_2O and (A) pre-reacted at 600 °C, (B) pre-reacted at 600 °C and washed in acetic acid and (C) pure $BaTiO_3$ + 3 wt.% $BaCO_3$.

liquid-phase sintering mechanism (Fig. 6). When the $BaCO_3$ phase was removed from the pre-reacted Li-doped $BaTiO_3$ powder by washing the powder with acetic acid the reaction kinetics was significantly slower and no sintering occurred at such a low temperature. In the next experiment the equivalent amount of $BaCO_3$ was added directly to undoped $BaTiO_3$ to exclude the formation of the oxygen vacancies but maintain the liquid phase. The sintering was again shifted to much higher temperatures, to the temperatures close to the sintering temperature of a pure $BaTiO_3$.

3.2. Mechanism of low-temperature sintering

Based on these experimental results we have developed a general explanation for the low-temperature sintering mechanism, called here reactive liquid-phase sintering, which we have tested and verified on a number of different compounds, including on those with very different crystal-chemistry characteristics.

The essential element of reactive liquid-phase sintering is the presence of a low-temperature liquid phase that must be able to directly or indirectly accelerate a reaction with the matrix phase. The following relationship[12] describes the rate of reagent conversion, where G is the degree of conversion, τ is the time, and C_1 and C_2 are the concentrations of the reagents:

$$\frac{dG}{d\tau} = KC_1C_2F$$

If we assume the same thermal conditions and the same reaction-limiting process, which is the rate of diffusion through the solid reaction layer, the coefficient K is approximately the same for the reaction between two solids or the reaction between a liquid and a solid. The rate of the reaction depends only on the surface contact areas (F), which in the case of the reaction between a liquid and a solid is significantly larger. So, if thermodynamic conditions for the reaction are ensured the rate of the reaction will be significantly increased when one of the reagents melts. The next contribution to the increased rate of the reaction in the presence of a liquid phase can be an appearance of a new mass-transport mechanism. The reaction rate would increase

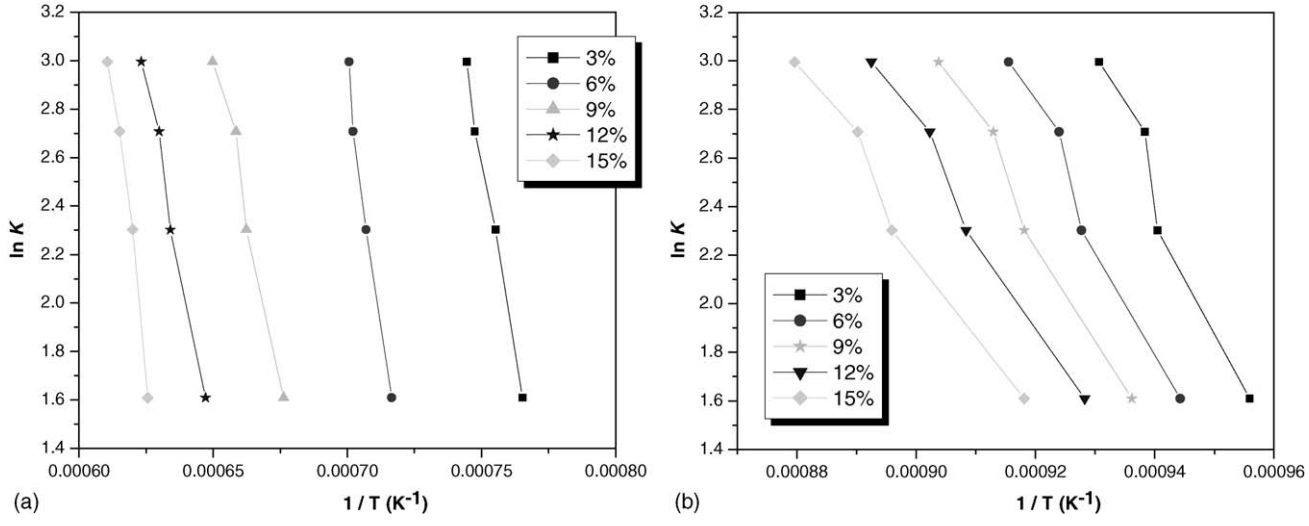

Fig. 5. The sintering rate (ln k) plotted against the inverse of temperature (1/T) for specific shrinkage values for undoped (A) and doped (B) $BaTiO_3$.

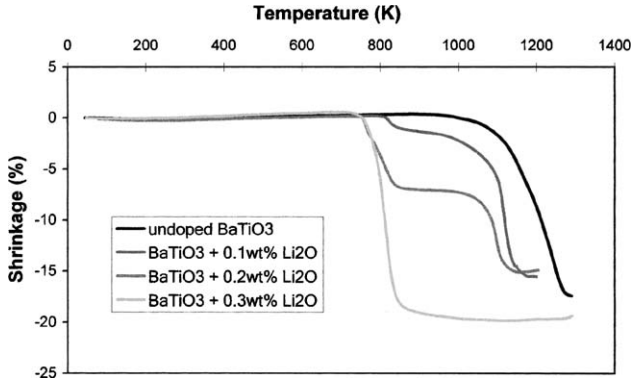

Fig. 7. Dynamic sintering curves of the $BaTiO_3$ powder, pre-reacted at 600 °C, as a function of Li_2O concentration (heating rate of 10 K/min). The sintering curves show the appearance of the new sintering mechanism at approximately 800 °C, which, for an addition of 0.3 wt.% Li_2O, fully controls the sintering behavior.

when the reactants would dissolve in the liquid phase and the product would precipitate.

The next important element of reactive liquid-phase sintering is the nature of the reaction with the matrix phase. The reaction must enhance at least one of three mass-transport processes, which are dominant in such a system during sintering. The most direct way is to increase the ion lattice-diffusion coefficient. The lattice-diffusion coefficient is proportional to the vacancy concentration; as a result, the sintering rate will increase when the structural vacancies are generated during the reaction with the matrix phase. The process called a liquid-phase (-assisted) sintering, where the mass transport goes through the liquid phase by a solution-precipitation method, also promotes the sintering. This process can be further accelerated by an increase in the solubility of the matrix phase during or after the reaction. Finally, if during the reaction with the matrix phase a temporary or permanent amorphization occurs a viscous flow from the grain surface to the necks between the grains contributes to the sintering.

In the case of Li_2O-doped $BaTiO_3$ the melted $BaCO_3$ indirectly accelerates a reaction with the matrix phase by releasing Li_2O during the reaction with Li_2TiO_3. Our experiments confirmed that the presence of the flux and the simultaneous reaction of Li_2O with the matrix phase increases the kinetics of two mass-transport processes during the low-temperature sintering. Fig. 7 shows the sintering behavior of $BaTiO_3$ powders doped with different concentrations of Li_2O from 0 to 0.3 wt.%. For the samples with 0.1 and 0.2 wt.% Li_2O a two-step sintering regime is obvious. During the first, low-temperature, step a reactive liquid-phase sintering takes place; the process described above. During this process the vacancies are generated in the matrix phase but the melted $BaCO_3$ is consumed during the reaction with TiO_2. When all the liquid phase is consumed the mass transport through the liquid phase cannot be realized anymore and the sintering is slowed down. Nevertheless, because of the presence of the oxygen vacancies in the matrix phase the lattice-diffusion coefficient is higher than for the undoped $BaTiO_3$. This is reflected in the second sintering step, which is accomplished at a lower temperature than for the undoped $BaTiO_3$. For the sample with 0.3 wt.% Li_2O the amount of $BaCO_3$ produced during the reaction is high enough so that the sintering is completed before all of it is consumed (see Fig. 1).

3.3. Generalization to other systems

In the second stage of our investigation we looked at many other systems. We applied the reactive liquid-phase sintering mechanism to successfully sinter a number of powders with very different chemistries although Li_2O was not always used as the sintering aid. The sintering aids were selected according to the crystal-chemistry of the matrix phase in such a way that they would trigger all the mechanisms required for the reactive liquid-phase sintering. In Table 1 these sintering experiments are listed together with the results of the studies of the reaction mechanisms and the sintering behavior. The corresponding sintering curves are shown in Fig. 8.

The analysis of the reaction and sintering mechanisms revealed that the addition of Li_2O to $(Ba,Sr)TiO_3$ ceramics activates very similar reaction and sintering mechanisms as in the case of $BaTiO_3$.[13] Again, the $BaCO_3$ flux forms as an intermediate reaction product and this increases the incorporation of Li_2O into the perovskite matrix. In the case of $SrTiO_3$ the $BaCO_3$ flux cannot form, therefore we added it together with Li_2O. For the determination of the activation energy for sintering the $(Ba_{0.6}Sr_{0.4})TiO_3$ powder with an addition of 0.4 wt.% Li_2O the same procedure was perfomed as in the case of $BaTiO_3$. For a comparison we measured a commercial, undoped 50 nm $(Ba_{0.6}Sr_{0.4})TiO_3$ powder and the results showed that the E_a of the powder is virtually double (587 kJ mol^{-1})[14] compared to the E_a value of doped $(Ba_{0.6}Sr_{0.4})TiO_3$ powder (297 kJ mol^{-1}).

Table 1
Parameters of the sintering experiments for which the reactive liquid-phase sintering was applied

Matrix compound	Sintering aid	Conc. (wt.%)	Flux	T (melt) (°C)	T (sint) (°C)	T (sint) undoped (°C)
$BaTiO_3$	Li_2O	0.3	$BaCO_3$	811	820	1250–1300
$(Ba,Sr)TiO_3$	Li_2O	0.4	$BaCO_3$	811	880	1300
$SrTiO_3$	$Li_2O + BaCO_3$	0.6 + 3.0	$BaCO_3$	811	1020	1350
TiO_2	CuO	0.2	CuO–TiO_2 eutectic	920	940	1300
Zn_2SiO_4	Li_2CO_3	0.2	Li_2CO_3	720	1050	1350
$AgNbO_3$	H_3BO_3	0.5	Ag-B glass	<450	950	1100
X7R	$Li_2O + BaCO_3$	0.6 + 3.0	$BaCO_3$	811	900	1090

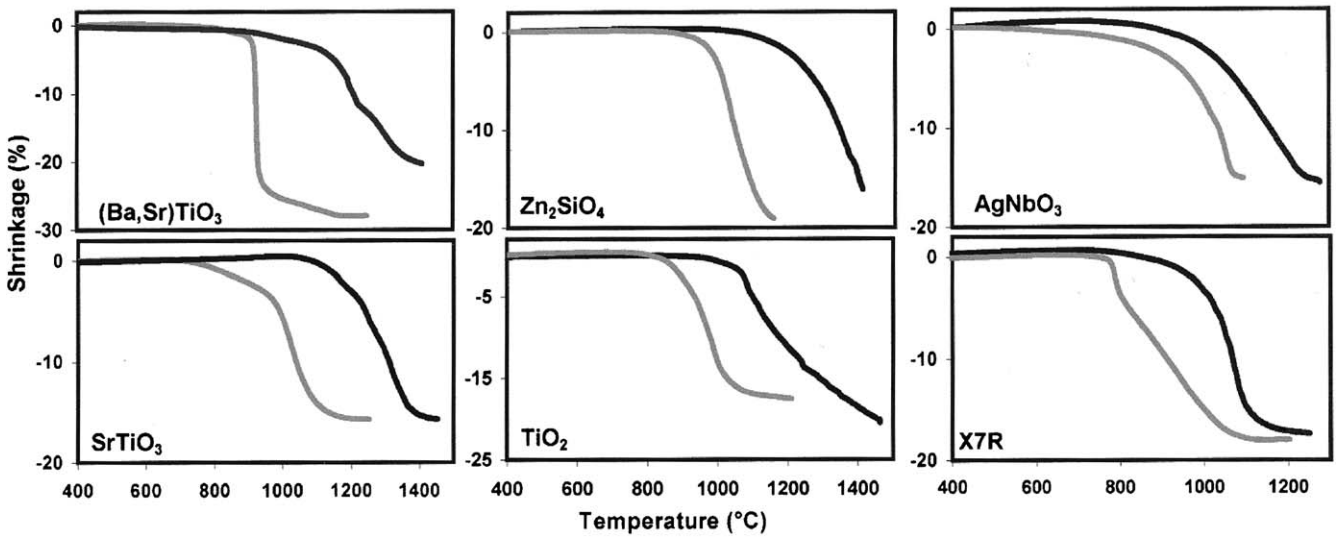

Fig. 8. A comparison of a sintering behavior of doped (red curves) and undoped powders (blue curves) from Table 1. The dynamic sintering curves were taken with a heating rate of 10 K/min.

The XRD and SEM analyses of the reaction and sintering mechanisms explained the low-temperature sintering of Zn_2SiO_4. Li_2CO_3 added to Zn_2SiO_4 melts at 720 °C; this accelerates the reaction with the matrix Zn_2SiO_4 phase; the substitution of Zn^{2+} with Li^+ and the consequent formation of oxygen vacancies, and the formation of ZnO secondary phase. As in other cases of reactive liquid-phase sintering, the synergetic influence of an increased lattice diffusion coefficient and the presence of a liquid phase significantly increases the sintering kinetics at low temperatures (1050 °C).

For the sintering of rutile TiO_2 we selected CuO as a sintering aid because of the existence of a low-temperature eutectic. The same experiments are already reported in the literature[15–17] and our results fully agree with them. Because the literature reports lack a detailed investigation and explanation of the sintering mechanism we performed these studies in the light of the proposed reactive liquid-phase sintering mechanism. The onset of the sintering closely corresponds to the melting temperature of the CuO–TiO_2 eutectic (920 °C).[18] After the flux is formed there are two processes activated that induce low-temperature sintering. The first is the so-called liquid-phase-assisted sintering, which is promoted by a high content of TiO_2 in the eutectic melt (∼16 mol%). The presence of the flux also promotes the incorporation of CuO in TiO_2 according to the already reported mechanism, $Ti_{1-x}Cu_xO_{2-2x}$ ($x < 0.004$).[19] This necessarily leads to the creation of the oxygen vacancies, which increases the lattice diffusion coefficient.

Silver-borate glasses have a softening temperature that, for the boron-rich compositions, increases with the silver content but remains below 450 °C.[20,21] This means that, when boric acid is added to $AgNbO_3$ it decomposes to a boron oxide, which during firing melts. The melt dissolves silver from the matrix phase and the matrix phase remains oxygen and silver deficient. The simultaneous presence of the liquid phase, an increase in the lattice diffusion coefficients and, most probably, also the enhanced viscous flow from the grain surface to the necks between the grains result in the low-temperature sintering of $AgNbO_3$.

Certainly, the addition of sintering aids has an influence on the physical properties of ceramics. However, the concentration of the sintering aid is small and in many cases it is entirely incorporated into the crystal lattice of the matrix. With the proper selection of sintering aid we can minimize the influence on the particular physical properties. An example is the commercial X7R capacitor formulation, which produces its desired dielectric properties as a result of an inhomogeneous core-shell microstructure. By applying the same method as for the $SrTiO_3$ (see Table 1) we managed to reduce the sintering temperature from 1090 to 900 °C. Due to the low processing temperature the inhomogeneity was well preserved, much better than during the regular sintering at 1090 °C, and consequently the obtained dielectric properties are even better than usual. In addition, due to such a low sintering temperature the expensive palladium can be eliminated from the electrodes of the X7R multilayer capacitors, which makes the production significantly cheaper.

4. Conclusions

An addition of just 0.3 wt.% of Li_2O to $BaTiO_3$ powder was able to reduce the sintering temperature to 820 °C, and ceramics with more than 95% of relative density can be produced. Small amounts of two secondary phases were formed during this process: Li_2TiO_3 and Ba_2TiO_4. A detailed study of the reaction mechanism between Li_2O and $BaTiO_3$ and the sintering behaviour revealed the main processes of the low-

temperature sintering, which we called reactive liquid-phase sintering. Dilatometric studies were performed to show the decrease in the activation energy for sintering obtained with this mechanism.

The required conditions to trigger the reactive liquid-phase sintering are: (i) the formation of a low-temperature liquid phase, (ii) a reaction with the matrix, which is accelerated by the liquid phase and (iii) the consequent enhancement of elementary sintering mechanisms. So, the lattice diffusion coefficient can be increased by the creation of vacancies or other point defects; the solubility of the matrix in the flux can enhance the mechanism of sintering based on the solution and precipitation of the matrix material; the viscous flow can be enhanced due to the temporary or permanent amorphisation or a decrease in the crystallinity.

The recognized low-temperature sintering mechanism was applied to several other materials and in all cases the sintering temperature was significantly reduced. On the commercial capacitor X7R formulation it was demonstrated that with a proper sintering-aid selection the relevant physical properties can be maintained, while some significant technological advantages can be obtained.

Acknowledgement

This work is supported by the European Competitive and Sustainable Growth Research Programme under Grant GRD1-2001–40547, EU Framework 5 project TUF.

References

1. Huassonne, J. M., Desgardin, G., Bajolet, P. H. and Raveau, B., Barium-titanate perovskite sintered with lithium-fluoride. *J. Am. Ceram. Soc.*, 1983, **66**, 801–807.
2. Wang, S. F., Yang, T. C. K., Huebner, W. and Chu, J. P., Liquid-phase sintering and chemical inhomogeneity in the $BaTiO_3$–$BaCO_3$–LiF system. *J. Mater. Res.*, 2000, **15**, 407–416.
3. Roulland, F., Terras, R. L., Allainmat, G., Pollet, M. and Marinel, S., Lowering of $BaB'_{1/3}B''_{2/3}O_3$ complex perovskite sintering temperature by lithium salt additions. *J. Euro. Ceram. Soc.*, 2004, **24**, 1019–1023.
4. Yang, Y., Feng, C. D. and Yu, Y. H., Low temperature sintering of PMN ceramics by doping with SrO. *Mater. Lett.*, 2001, **49**, 345–351.
5. Walker, B. E., Rice Jr., R. W., Pohanka, R. C. and Spann, J. R., Densification and Strength of $BaTiO_3$ with LiF and MgO Additives. *Am. Ceram. Soc. Bull.*, 1976, **55**, 274–285.
6. Tolino, D. A. and Blum, J. B., Effect of Ba–Ti ratio on densification of LiF-fluxed $BaTiO_3$. *J. Am. Ceram. Soc.*, 1985, **68**, C292–C294.
7. Desgardin, G., Mey, I., Raveau, B. and Haussonne, J. M., $BaLiF_3$—a new sintering agent for $BaTiO_3$-based capacitors. *Am. Ceram. Soc. Bull.*, 1985, **64**, 564–570.
8. Xu, B. M. and Yin, Z. W., Microstructure development of the single-step, low-temperature sintered $SrTiO_3$ GBBL capacitor material. *Ferroelectr. Lett.*, 1993, **16**, 157–165.
9. Randall, C. A., Wang, S. F., Laubscher, D., Dougherty, J. P. and Huebner, W., Structure property relationship in core-shell $BaTiO_3$–LiF ceramics. *J. Mater. Res.*, 1993, **8**, 871–879.
10. Barringer, E.A., *The Synthesis, Interfacial Electrochemistry, Ordering, and Sintering of Monodisperse TiO_2 Powder*. Ph.D. thesis, Massachusetts Institute of Technology, 1983, p. 187.
11. John, V. B., *Introduction to Engineering Materials* (*3rd ed.*). Macmillan, Houndmills, UK, 1992.
12. Budnikov, P. P. and Ginstling, A. M., In *Principles of Solid State Chemistry: Reactions in solids*, ed. K. Shaw. MacLaren and Sons Ltd., London, 1968. pp. 166–175.
13. Valant, M. and Suvorov, D., Low-temperature sintering of $(Ba_{0.6}Sr_{0.4})TiO_3$. *J. Am. Ceram. Soc.*, 2004, **87**, 1222–1226.
14. Sarma, K., Farooq, R., Jarman, K., Pullar, R. C., Petrov, P. K. and McN Alford, N., Sintering behaviour of $Ba_xSr_{1-x}TiO_3$. *Integr. Ferroelectr.*, 2004, **62**, 249–252.
15. Kim, D. W., Kim, T. G. and Hong, K. S., Low-firing of CuO-doped anatase. *Mater. Res. Bull.*, 1999, **34**, 771–781.
16. Kim, D. W., Park, B., Chung, J. H. and Hong, K. S., Mixture behavior and microwave dielectric properties in the low-fired TiO_2–CuO system. *Jpn. J. Appl. Phys.-Part*, 2000, **39**, 2696–2700.
17. Chang, J. C., Chen, Y. F. and Jean, J. H., Low-fire processing and dielectric properties of TiO_2 with MnO_x–CuO. *Jpn. J. Appl. Phys.*, 2004, **43**, 4267–4268.
18. Lu, F. H., Fang, F. X. and Chen, Y. S., Eutectic reaction between copper oxide and titanium dioxide. *J. Euro. Ceram. Soc.*, 2001, **21**, 1093–1099.
19. Shannon, R. D. and Pask, J. A., Kinetics of anatase-rutile transformation. *J. Am. Ceram. Soc.*, 1965, **48**, 391–398.
20. Boulos, E. N. and Kreidle, N. J., Structure and properties of silver borate glasses. *J. Am. Ceram. Soc.*, 1971, **54**, 368–375.
21. Piguet, J. L. and Shelby, J. E., Preparation and properties of silver borate glasses. *J. Am. Ceram. Soc.*, 1985, **68**, 450–455.